

# Exploring the Remapping Impact of Spatial Head-hand Relations in Immersive Telesurgery

ANONYMOUS AUTHOR(S)

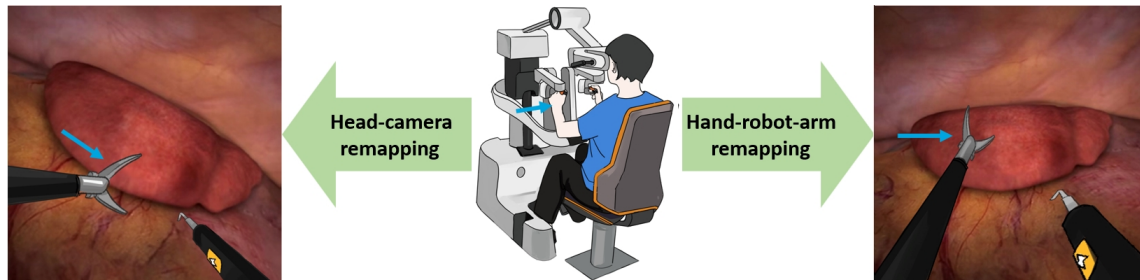


Fig. 1. Schematic diagram of immersive telesurgery system and the remapping situations of spatial head-hand relations it often faces

When skilled surgeons are not available at the hospital and surgery is required, the immersive telesurgery system offers a mainstream and effective solution. The operator can observe through the robot's camera and use their hands to control the robot-arms, as if they were the robot. However, common remapping of spatial head-hand relations—due to camera adjustments and robotic arm switching—creates significant visual-proprioceptive conflicts and physical limitations. To explore this, we simulated an immersive telesurgery system and set remapping conditions and situations: head-camera remapping with 6 situations and hand-robot-arm remapping with 12 situations. We assessed their perception and behavior effects across four typical surgical tasks: navigation, location, cutting, and bimanual coordination. The study evaluates spatial perception bias, interactive deviation, workload, and task completion time. Our findings reveal how different remapping targets, attributes, intensities, and situations affect performance, contributing to the understanding of perception mechanisms and offering insights for optimizing operations or systems.

CCS Concepts: • **Human-centered computing** → **User studies**; **Virtual reality**.

Additional Key Words and Phrases: Immersive telesurgery, Spatial perception, Remapping, Sensory conflict

## ACM Reference Format:

Anonymous Author(s). 2018. Exploring the Remapping Impact of Spatial Head-hand Relations in Immersive Telesurgery. In *Proceedings of Make sure to enter the correct conference title from your rights confirmation email (Conference acronym 'XX)*. ACM, New York, NY, USA, 23 pages. <https://doi.org/XXXXXXXX.XXXXXXX>

## 1 Introduction

Despite advancements in artificial intelligence, autonomous robots still cannot match human intuition and reasoning, especially in tasks requiring experience and specialized skills [13, 48]. While control algorithms can handle complex interactions, humans excel in kinematics, efficiently performing such tasks in daily life [7, 46]. When skilled surgeons aren't available locally, immersive telesurgery becomes a key solution, particularly for procedures requiring high

---

Permission to make digital or hard copies of all or part of this work for personal or classroom use is granted without fee provided that copies are not made or distributed for profit or commercial advantage and that copies bear this notice and the full citation on the first page. Copyrights for components of this work owned by others than the author(s) must be honored. Abstracting with credit is permitted. To copy otherwise, or republish, to post on servers or to redistribute to lists, requires prior specific permission and/or a fee. Request permissions from [permissions@acm.org](mailto:permissions@acm.org).

© 2018 Copyright held by the owner/author(s). Publication rights licensed to ACM.

Manuscript submitted to ACM

Manuscript submitted to ACM

53 precision and expertise in complex environments [5, 62]. This method, widely used and studied in both industry and  
54 academia, allows remote surgeons to control surgical robots through VR headsets and handheld controllers, merging  
55 their hand movements with robotic arm actions as if they were their avatars [9, 28]. The VR headset is usually fixed to  
56 minimize physical effort and motion sickness during long surgeries, providing stable head support. Foot pedals control  
57 binocular camera movement. The operator can manage 3 to 5 robotic arms with different instruments, controlling two  
58 at the same time and switching between them as needed [9, 10, 36].

59 However, this control method often leads to remapping the spatial head-hand relation, disrupting the alignment  
60 between the operator’s head-hands and camera-robotic-arms, which creates significant visual-proprioceptive conflicts  
61 and physical limitations. This is for two reasons. On the one hand, operators frequently need to move or rotate the  
62 camera to avoid internal structures like organs, tissues, or nerves, or to maintain a clear, unobstructed view of the  
63 surgical site. On the other hand, switching between robotic arms can cause a mismatch between the operator’s hand  
64 position/rotation and the robotic arm’s position/rotation. Unlike continuous remapping in VR, like haptic repositioning  
65 or walking redirection, this remapping is discrete, applying one-time offset and deflection at specific moments—such  
66 as before a procedure or when switching robot-arms. This discrete remapping may affect the operator’s perception,  
67 cognition, and actions, yet its impact is still underexplored.

71 In our study, we used VR to simulate both the operator and robot sides of a telesurgery system. We implemented  
72 head-camera and hand-robot-arm remapping based on remapped target objects, creating three experimental conditions,  
73 including the aforementioned two remappings and a control condition without remapping. To more comprehensively  
74 and precisely assess the impact of sensory conflict, we introduced positional offsets and rotational deflections to the  
75 camera and robotic arms in different directions, generating 18 remapping situations. We then evaluated the effects of  
76 these remapping conditions and situations through 4 key surgical tasks: navigation with obstacle avoidance, spatial  
77 location, cutting based on spatial perception, and bimanual coordination surgery. Our evaluation combined both  
78 subjective and objective measures to assess spatial perceptual bias rate, interactive action deviation, workload, and task  
79 completion time. The experimental results show that when the remapping target is head-camera, it has the greatest  
80 impact on spatial perception bias, especially in cases where the remapping attribute and intensity are strong deflection.  
81 On the other hand, when the remapping target is hand-robot-arm, it has the greatest impact on physical limitations and  
82 load, particularly in cases where the remapping attribute and intensity are strongly offset. We speculate that this is  
83 due to the combined effect of the visual-proprioceptive conflict caused by the remapping and the physical limitations  
84 imposed by compensatory actions.

85 This study holds three key implications: First, it deepens our understanding of the performance effects and perception-  
86 cognition-behavior mechanisms in the remapping of spatial head-hand relations. Second, it provides valuable insights  
87 for surgeons and trainees on how to adjust head-hand spatial relations during procedures to mitigate or accelerate  
88 adaptation to sensory conflicts. Third, it offers guidance for the functional design, effective optimization, and sensory  
89 intervention strategies of immersive teleoperation systems. To our knowledge, this is the first study to define the  
90 visual-proprioceptive conflicts and physical limitations arising from the remapping of spatial head-hand relations. Our  
91 contributions include: i) Systematically revealing how different remapping targets (head-camera and hand-robot-arm),  
92 attributes (offset and deflection), and offset/deflection parameter size (strong and weak) affect spatial perception and  
93 interactive behavior. ii) Speculating the underlying perception-to-behavior mechanisms that drive these effects based  
94 on sensory integration theory. iii) Ranking the remapping situations by the impact levels, identifying those that require  
95 attention, avoidance, or intervention.

## 2 Related Work

This study focuses on exploring remapping impact in immersive telesurgery systems, closely related to immersive teleoperation systems and VR remapping, and relying on theories of sensory integration and conflict mechanisms.

### 2.1 Immersive Teleoperation Robotic System

Immersive teleoperation robotic systems show great potential in unstructured, dynamic, and complex environments, particularly for tasks requiring flexible hand-eye coordination, object recognition, and obstacle detection [82]. Operators control robots remotely from a first-person perspective, without focusing on the mapping between user inputs and robot actions. This egocentric control method transfers human-level cognitive and motor skills to robotic systems [4, 95, 96]. However, like avatar control in VR, embodied interaction presents challenges in perception, cognition, and behavior. Research has added haptic feedback to controllers to address the lack of tactile sensation [1, 29], used speed remapping on robotic arms to create pseudo-haptic illusion and alter weight perception [70], studied the effects of body tilt and environmental information on spatial awareness [50, 90], explored the differences between first- and third-person perspectives [97], compared 2D and 3D interfaces for depth perception [81], and examined the impact of latency on robot responsiveness [15].

Immersive teleoperated robots are widely used in surgeries like laparoscopy, thoracoscopy, and neurosurgery, allowing operations without local skilled surgeons and filtering out hand tremors [5, 27, 51, 63, 86]. These systems fix the operator's head to a 3D display, and the crowded internal structure limits movement, posing challenges like reduced sensory feedback, motion sickness, and visual fatigue [22, 32, 80, 85, 89]. This hinders surgeons' hand-eye coordination [93] and increases their cognitive and physical load [25, 65, 86].

These challenges on immersive teleoperated systems inspire us to focus on this critical area, particularly the impact of perception-to-behavior. These findings also drive us to explore the underexamined issue of spatial remapping in immersive telesurgery.

### 2.2 VR Remapping

In virtual reality (VR), remapping techniques are widely used to manipulate visual perception, allowing users to perform tasks where physical translation/rotation/size don't exactly align with those in the virtual space. This enhances user capabilities and creates intriguing illusions [6, 42]. Remapping involves calculating the gain between virtual and real-world objects, including offset (where the virtual object is mapped to an additional position) and deflection (where the virtual object has additional rotation) [52].

Gains can be continuous or discrete, depending on how frequently they are applied. Continuous gains respond to ongoing changes in the physical world. For example, curvature/bending-based walking redirection alters the physical path's curvature to allow users to walk through larger virtual environments within limited physical space [11, 47, 75, 77]. Haptic retargeting [66, 75] enhances the VR experience by dynamically manipulating visual and tactile perception. Jumping Redirection [35, 39] improves user locomotion capabilities in VR. Similarly, head-turning redirection [60] allows users to view wider virtual spaces, and action speed remapping adjusts perceptions of weight and time [73, 74].

Discrete gains occur once at specific trigger chance. For instance, upright and swimming redirection [16, 57, 91] adjusts body posture and orientation to allow users to engage in more VR interactions. Body and arm rescaling enhance users' locomotion and action range by enlarging their virtual body size and arm length, respectively [2, 42].

157 Similarly, the remapping of head-hand relations is a discrete remapping technique. Unlike intentional VR remappings,  
158 remapping of head-hand relations in immersive telesurgery is often forced to meet the necessary needs, such as obstacle  
159 avoidance or switching robotic arms. Given the seriousness of surgical settings, the consequences of such remapping  
160 can be more severe, making it essential to explore its impact in detail.  
161

### 162 **2.3 Sensory Integration and Conflict**

163 The brain integrates multisensory information from various parts of the body to form perceptions of self and spatial  
164 awareness [68]. Visual factors such as color, occlusion, depth, and motion flow significantly influence our spatial  
165 judgments [58, 59]. The vestibular system, which senses linear acceleration, gravity, head position, and angular  
166 velocity [79], has a substantial impact on visual-spatial abilities, including spatial memory, navigation, mental rotation,  
167 and mental representation of three-dimensional space [18, 26, 67]. This sensitivity is notably affected by the angle  
168 of head tilt and gravity [3]. Proprioceptors, such as muscle spindles and tendon organs, provide crucial information  
169 about muscle length and tension, joint position changes, and are essential for perceiving the position, movement, and  
170 posture of body parts [14]. The brain weights each type of sensory information based on its reliability to derive the  
171 most accurate perceptual result [23, 24, 55]. Finally, the brain takes into account previous experiences and current  
172 intentions to optimize decision-making [8, 53, 72].  
173

174 In spatial interactions, users experience complex multisensory integration [42]. Even if not consciously aware,  
175 vestibular and proprioceptive inputs are vital in VR environments [71]. For example, users can easily perceive the  
176 position and angle of their head, arms, and fingers even with their eyes closed. Integrating multiple sensory cues  
177 generally yields more accurate spatial judgments than relying on a single cue. For example, without vestibular and  
178 proprioceptive feedback, users may underestimate distances based solely on visual cues [41]. Conversely, without visual  
179 information, relying only on vestibular and proprioceptive feedback can reduce distance estimation accuracy [94].  
180 Perceptual integration theory suggests that multisensory conflicts in VR can lead to spatial disorientation, simulator  
181 sickness [30, 45], and reduced body ownership [69].  
182

183 The characteristics of the three senses have led us to confirm the type of sensory conflict addressed in this study,  
184 which is visual-proprioceptive conflict. This is due to immersive telesurgical systems having a fixed head position,  
185 without changes in head angle affecting vestibular sensitivity, and without visual motion that would significantly  
186 conflict with static vestibular perception. Moreover, the theory of sensory integration and conflict provides a crucial  
187 basis for speculating the perception-to-behavior mechanisms of remapping.  
188

## 189 **3 Design Considerations and Pilot Experiment**

190 This section enhances the formal experiment’s design by introducing considerations for the immersive telesurgery  
191 system’s simulated method and common remapping situations. It also outlines suitable remapping offset/deflection  
192 parameters based on results from a pilot experiment.  
193

### 194 **3.1 Considerations for Simulated Immersive telesurgery System**

195 We reviewed 16 commercial immersive telesurgery systems, including Da Vinci 5 [83], Hinotori [19], BITRACK  
196 SYSTEM [84], SSi Mantra [56], Hugo RAS [61], etc. Of these, five systems (31.25%) use a fixed downward-angled 3D  
197 display to simulate a typical surgical view, with arm interactions in both vertical and horizontal planes (Figure 2(a)).  
198 The remaining eleven systems (68.75%) use a horizontally fixed 3D display, offering a more standard view and improved  
199 neck comfort, with interactions mainly in the vertical plane (Figure 2(b)).  
200

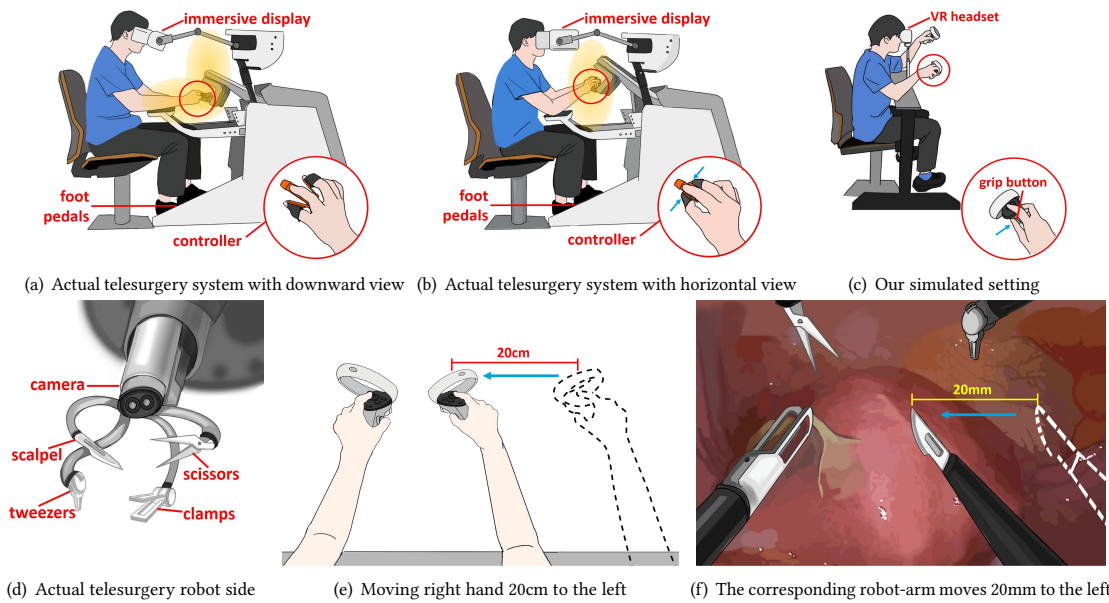


Fig. 2. Configurations for simulating immersive telesurgery system

For simulating these immersive telesurgery systems, we chose the more common horizontal view setup for user experiment to minimize physical fatigue and dispersed interactive actions. On the operator side, a narrow table was used to simulate arm support, with a stand fixing the VR headset in a forward-facing position (Figure 2(c)). We also designed a grip posture for the VR handles to closely replicate surgical controllers, using the 'Grip' button to simulate surgical controller actions for opening/closing clamps, tweezers, or scissors. Since remapping of head-hand relations and robotic arm switching were automated by our system, foot pedal controls for camera adjustments and robot-arm switching were not included.

Actual surgical robots typically have one binocular camera and four robotic arms, each equipped with different tools (Figure 2(d)). On our robot side, we used four robotic arms fitted with common instruments including scalpel, clamps, scissors, and tweezers. Participants controlled two arms at a time, with the robotic arms' movements directly mirroring the operator's hand motions. Given the small size of surgical targets, the surgical robot size and speed mapping were also scaled down for operational precision. Usually, the robotic arm movement is mapped to be one-fifth to one-fifteenth of the operator's hand speed. For the formal experiment, we set the hand-to-robotic-arm speed ratio at 10:1 to avoid cognitive load, meaning a 20 cm arm movement corresponds to a 20 mm robotic arm movement (Figure 2(e) and (f)). This way, participants could intuitively perceive distances/angles by visual and proprioceptive actions, and mentally converting centimeters to millimeters, maintaining the natural spatial awareness in daily life. The scaled movements in the camera view appeared consistent with hand motions in the eye view, maintaining the spatial head-hand relationship.

### 3.2 Considerations of Remapping Situations

We analyzed 52 videos of immersive telesurgical systems in use, either during surgeries or training, on platforms like YouTube. We found that 44 of them (84.6%) involved remapping of spatial head-hand relations, indicating the prevalence of this phenomenon. First, we observed that the head remains fixed, while the camera's position and rotation are frequently adjusted to accommodate different surgical scenarios or personal preferences, leading to frequent

261 head-camera remapping. For example, when the spatial height is low, the camera needs to offset downward; to better  
262 observe small lesions, cysts, tumors, or nodules, the camera is offset forward; when a large lesion area requires wide  
263 hand movements, the camera is offset back to provide a broader view. Additionally, to make the flat binocular camera  
264 fit in a narrow gap or adjust the tilted object in the view to be straight, the camera may be rolled deflection. Another  
265 common occurrence is remapping due to switching control between robotic arms. Since the hand may be in any position  
266 or angle when switching to a new set of robotic arms, and the robotic arms remain in their last controlled positions and  
267 rotations, possible mismatched situations between the hand and robotic arms are various.

268  
269 Based on these 2 types of head-hand spatial relationships, we set 2 remapping conditions: head-camera remapping  
270 and hand-robot-arm remapping. To comprehensively cover potential remapping cases during surgery, we further divide  
271 the conditions into 18 specific remapping situations, categorized by the remapping attribute (offset or deflection) and  
272 its direction (left/right, up/down, and forward/backward). These include 6 head-camera remapping situations (columns  
273 2 and 3 in Table 1) and 12 hand-robot-arm remapping situations (columns 2 and 3 in Table 2). Since there are two hands,  
274 we distinguish between symmetric and asymmetric offsets/deflections of the robotic arms, resulting in more situations.  
275 It's worth noting that a camera offset to one direction differs from the offset of two robotic arms in opposite directions,  
276 as the camera's offset affects the view, whereas the robotic arms' offset does not.  
277  
278  
279  
280

### 281 3.3 Pilot Study

282 The pilot experiment aimed to optimize remapping parameters for the formal experiment and reduce potential confound-  
283 ing factors. We recruited 10 participants (5 male, 5 female, average age = 25.6, SD = 2.46, age range: 22-30) from 3 local  
284 universities, all with HCI research backgrounds and thus more attuned to user experience and parameter selections.

285 According to the common remapping parameters, we set five ranges for positional offset and rotational deflection  
286 for each remapping condition (second-to-last column in Tables 1 and 2). Participants experienced each range in a  
287 counterbalanced order in the formal experiment scene and selected the most suitable parameters. We counted the  
288 number of participants' selections, and the most frequently chosen ranges were set as the final remapping parameters  
289 (first-to-last column in Table 1 and 2). Among interviews, seven participants found hand-robot-arm remappings with  
290 big parameters introduced unrelated factors like huge physical strain, while eight felt head-camera remappings with  
291 big parameters caused poor visibility of the surgical site. Six believed parameters with small parameters were hard to  
292 perceive and unfavorable for research, and eight preferred moderate remapping parameters (i.e., not big and not small)  
293 as they better reflected actual situations.  
294  
295  
296  
297  
298

## 299 4 User Study

300 This study explores how various remappings of spatial head-hand relations affect participants' spatial perception and  
301 interaction behavior during typical surgical tasks.  
302  
303

### 304 4.1 Ethics and Participants

305 The experiment was approved by our university's ethics committee, excluding individuals with sensory, cognitive, or  
306 motor impairments. we did not recruit professional surgeons, since the tasks were simple and required no medical  
307 knowledge or skills, all participants could perform the tasks proficiently after practice. We recruited 20 students (10  
308 male, 10 female; average age = 24.6, SD = 2.50, age range: 21-29) from three local universities. Six participants were  
309 highly experienced with VR, seven had moderate experience, and seven were novices. Additionally, five participants  
310  
311

were familiar with the concept of immersive telesurgery systems by advertisements and videos but had no practical usage experience.

#### 4.2 Scenario and Experimental Tasks

We designed an abstract experimental scenario and four general tasks based on literature and videos in Sections 3.1 and 3.2. These tasks are not tied to any specific surgery but are applicable to a variety of procedures. The abstract scenario and general tasks offer broad applicability while simplifying the system's interface and avoiding the need for medical expertise, thereby reducing participants' cognitive load. The virtual surgical environment we created includes a series of interlocking convex and flat surfaces to simulate complex internal environments, with irregularly shaped organs, tissues, and lines representing blood vessels and nerves, as shown in Figure 3. These structures are densely packed, replicating the narrow, confined space typical of surgical procedures. We modeled four virtual robotic arms, equipped with scalpel, tweezers, scissors, and clamps.

Additionally, we developed four typical, general surgical tasks to simulate the essential steps in locating and removing tumors/cysts/nodules:

**Task 1-Navigation and Obstacle Avoidance:** This task simulates the operator controlling the robot arms to move within the body while avoiding critical structures like organs, blood vessels, nerves, and tissues [44, 78, 88]. Participants control two robotic arms to navigate through a confined space, avoiding critical structures to reach the target tissue. A visualized optimal path guides participants to ensure consistent obstacle avoidance for later evaluation, as shown in Figure 3(a).

Table 1. Configurations of head-camera remapping based on design considerations and pilot experiment


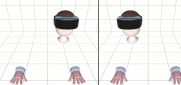
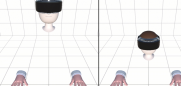
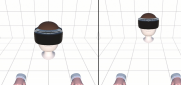
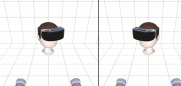

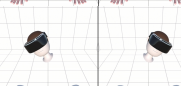
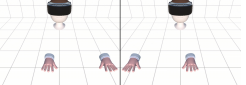
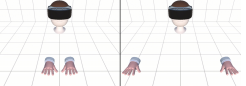
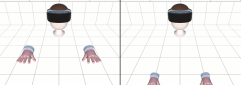
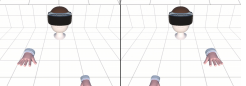
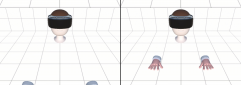
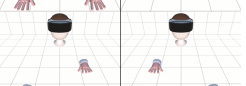
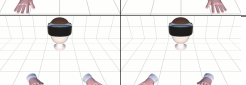
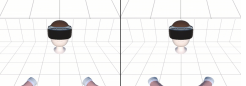

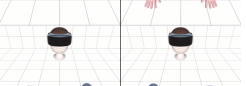

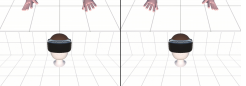
Condition	Situation	Diagram	Optional offset/ deflection	Determined offset/ deflection
No remapping	No offset and deflection (NOD)		/	/
Head-camera remapping	Camera is offset to left/right (COL/R)		2mm-6mm(1) 3mm-9mm(2) 5mm-15mm(6) 7mm-21mm(1) 9mm-27mm(0)	5mm-15mm
	Camera is offset to up/down (COU/D)			
	Camera is offset to forward/ backward (COF/B)			
	Camera deflects to left/right (CDL/R)		5°-15°(1) 10°-30°(4) 15°-45°(2) 20°-60°(2) 30°-90°(1)	10°-30°
	Camera deflects to up/down (CDU/D)			
	Camera deflects to clockwise/ counterclockwise (CDC/C)			

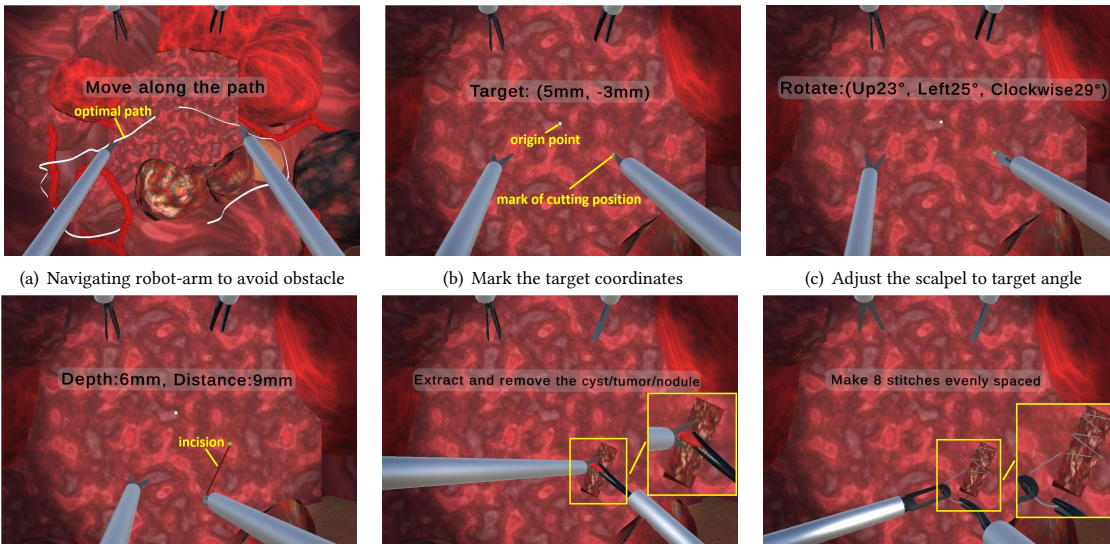
Table 2. Configurations of hand-robot-arm remapping based on design considerations and pilot experiment

Condition	Situation	Diagram	Optional offset/ deflection	Determined offset/ deflection
Hand-robot-arm remapping	Two robot-arms are <b>offset to left/right (ROL/R)</b>			
	One robot-arm is <b>offset to left</b> , the other to <b>right (ROL-R)</b>			
	Two robot-arms are <b>offset to up/down (ROU/D)</b>		2mm-6mm(0) 3mm-9mm(2) 5mm-15mm(5) 7mm-21mm(2) 9mm-27mm(1)	5mm-15mm
	One robot-arm is <b>offset to up</b> , the other to <b>down (ROU-D)</b>			
	Two robot-arms are <b>offset to forward/backward (ROF/B)</b>			
	One robot-arm is <b>offset to forward</b> , the other to <b>backward (ROF-B)</b>			
	Two robot-arms <b>deflect to left/right (RDL/R)</b>			
	One robot-arm <b>deflects to left</b> , the other to <b>right (RDL-R)</b>			
	Two robot-arms <b>deflect to up/down (RDU/D)</b>		5°-15°(1) 10°-30°(5) 15°-45°(3) 20°-60°(1) 30°-90°(0)	10°-30°
	One robot-arm <b>deflects to up</b> , the other to <b>down (RDU-D)</b>			
	Two robot-arms <b>deflect to clockwise/counterclockwise (RDC/C)</b>			
One robot-arm <b>deflects to clockwise</b> , the other to <b>counterclockwise (RDC-C)</b>				

**Task 2- Spatial Location:** This task simulates the operator locating a hidden tumor, cyst, or nodule beneath the surface of an organ based on the guiding data of medical images [20, 31, 54, 92]. The system provides a visible white origin point on the organ and a 2D coordinate relative to the origin for guiding the cutting position. Participants estimate the location using visual inspection (visual cues) and action measure (proprioceptive cues) and mark the cutting position (green point) with the tip of a scalpel, as shown in Figure 3(b).



**Task 3- Cutting based on Spatial Perception:** To minimize harm, this task focuses on accurately controlling the cutting angle, depth, and length to avoid blood vessels, nerves, and other vital points according to the guiding data of medical images [33, 37]. Participants control a scalpel to make an incision at the mark position, following system prompts for the insertion angle (randomly  $10^{\circ}$ - $30^{\circ}$  in various directions) and cut the tissue at a specified depth (randomly 4-8mm) and length (randomly 5-10mm), as shown in Figure 3(c) and (d).



(d) Insert and incise to target depth and distance (e) Extract and remove the cyst/tumor/nodule (f) Suture incision with 8 stitches evenly spaced

Fig. 3. Experimental scenario and task procedures

**Task 4- Bimanual Cooperation:** Simulating the removal of tumor/cyst/nodule and suturing the incision [37, 38, 40], participants use both hands for this task. The right robot arm, equipped with tweezers, holds the incision open to expose the tumor/cyst/nodule, while the scissors in the left robot arm cut it free (Figure 3(e)). Afterward, the left robot arm is automatically switched to clamps holding the suture needle, and participants must collaborate with both hands to stitch the wound evenly, as shown in Figure 3(f). The system automatically calculates the standard suture template trajectory based on the incision size and direction for subsequent evaluation.

### 4.3 Remapping Conditions and Situations

Following Section 3.1, we developed a VR-based teleoperation surgery system. The setup in the operator side includes an adjustable table and VR headset stand to suit participants of varying heights, and a new VR handle holding posture to simulate the actual surgical controlling. On the robot side, we reduced the size and speed of surgical robots to one-tenth of that of operators. Typically, users manually switch robotic arms, causing remapping. In our experiment, to avoid extra hand-robot-arm remapping caused by manual switching, the system automatically swaps the corresponding virtual robot arms when a tool change is needed.

Based on Section 3.2, we set two remapping conditions: head-camera remapping and hand-robot-arm remapping, along with a control condition without remapping. According to Tables 1 and 2, each remapping condition was further divided into more remapping situations (6 in head-camera and 12 in hand-robot-arm), with random offset (5-15mm on simulated robot side) or deflection values ( $10^{\circ}$ - $30^{\circ}$ ). These parameters ensured interaction actions weren't distorting or complicating, and the interaction area remained visible, minimizing unrelated variables.

Figure 4 illustrates the two situations of head-camera remapping and four situations of hand-robot-arm remapping during Task 4. For example, when the camera is offset 15mm forward, the robot arm appears bigger in the view (Figure 4(a)). Notably, the remapping of head-hand relations induces visual-proprioceptive conflicts, requiring either eye or hand compensation to complete the same robot action accurately. For example, in the situation where the camera deflects down 30°, participants need to rotate their eyes upward by 30° to clearly see the operational area (Figure 4(b)). When both robotic arms are offset forward by 15mm, participants need to move their hands 15cm backward to keep the robotic arms aligned with the incision (Figure 4(c)). Similarly, when both robotic arms deflect upward by 30°, participants need to rotate their hands downward by 30° to maintain precise operation in view (Figure 4(d)).

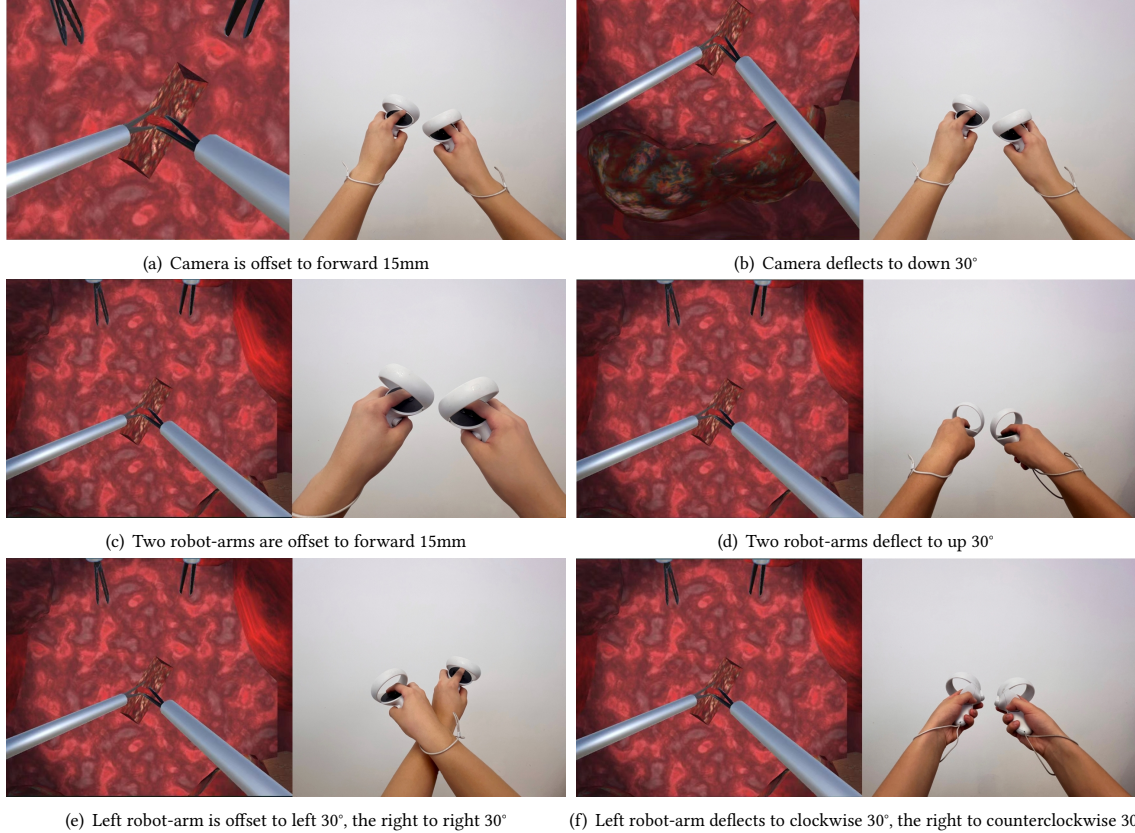


Fig. 4. Remapping situations cause mismatches between visual and proprioceptive actions.

#### 4.4 Evaluation Metrics

To objectively and subjectively measure the remapping impact of spatial head-hand relations, we established four metrics to assess spatial perception and behavior performance.

**4.4.1 Trajectory Deviation.** The system calculates navigation and suturing trajectory deviations for Task 1 and Task 4 using the Dynamic Time Warping (DTW) algorithm, known for its flexibility in handling sequences of varying lengths and local speed changes [76]. By comparing participants' trajectories with template trajectories, DTW calculates the average deviation value of each pair of sampling points.

4.4.2 *Perceptual Bias Rate.* In Task 2, the location bias rate (i.e.,  $br_l$ ) is calculated based on the difference between the participant's marked incision point ( $x, y$ ) and the system's target coordinates ( $x', y'$ ). In Task 3, the angle, depth, and distance bias rates (i.e.,  $br_a, br_d, br_D$ ) are determined using the difference in insert angles ( $\alpha, \beta, \gamma$ ), insert depth ( $d$ ), and incision distance ( $D$ ) compared to their respective target values ( $\alpha', \beta', \gamma'$ ),  $d', D'$ . The calculation method is shown in Formula 1.

$$\begin{cases} br_l = \frac{1}{2} \left( \frac{|x-x'|}{|x'|} + \frac{|y-y'|}{|y'|} \right) \\ br_a = \frac{1}{3} \left( \frac{|\alpha-\alpha'|}{\sqrt{|\alpha'|^2+|\beta'|^2+|\gamma'|^2}} + \frac{|\beta-\beta'|}{\sqrt{|\alpha'|^2+|\beta'|^2+|\gamma'|^2}} + \frac{|\gamma-\gamma'|}{\sqrt{|\alpha'|^2+|\beta'|^2+|\gamma'|^2}} \right) \\ br_d = \frac{|d-d'|}{|d'|} \\ br_D = \frac{|D-D'|}{|D'|} \end{cases} \quad (1)$$

4.4.3 *Workload.* We used the NASA-TLX to assess six dimensions of workload: mental demand, physical demand, temporal demand, performance, effort, and frustration, with each dimension scored on a scale of 0 to 20 [34]. This scale captures participants' perception and behavior effort when facing remappings.

4.4.4 *Task Completion Time.* The system automatically recorded the time taken to complete each task, excluding time spent filling out NASA-TLX. Completion time provides an objective measure of the effect on reaction and action time during remapping.

## 4.5 Procedure and Bias Mitigation

This experiment used a repeated measures design where each participant completed all remapping conditions and situations. There were 6 head-camera, 12 hand-robot-arm situations, and 1 control condition (no remapping). To balance various situation numbers in conditions (6 in head-camera condition, 12 in hand-robot-arm condition, and 1 in no remapping condition), the situations in head-camera condition were repeated twice, and the situation in no remapping condition was repeated 12 times.

Participants first practiced under the no remapping condition until they were familiar with the scenes and tasks. They then experienced each remapping scenario in a balanced order, aiming to complete the four tasks as quickly and accurately as possible. After each condition, participants filled out the NASA-TLX and provided feedback. Upon completing all scenarios, they participated in an interview.

Prior to the experiment, participants received a detailed introduction covering immersive telesurgery, remapping, procedures, and NASA-TLX. A pre-recorded demo video explained the tasks, and any questions were addressed to ensure familiarity. During practice, participants were trained to adapt to the robot avatar being 10 times smaller than their body, immediately converting perception measurements between centimeters (operator side) and millimeters (robot side) as needed. To mitigate potential effects from repeated measures and learning, the order of conditions was counterbalanced. Participants rested between conditions and situations until any subjective mental or physical fatigue subsided, and verbal confirmation was given that they were ready to proceed.

## 4.6 Implementation

Blender v3.6 was used to create 3D models of the robotic arms and surgical scenes, while Unity Engine v2021.3.32f1c1 was used to develop the four surgical tasks and control the experimental process. Participant and system data were

573 stored in JSON files. The remapping was implemented by applying an additional offset and deflection to the mapping of  
 574 the headset and handles in VR. The experiment utilized Oculus Quest 2 [87] as the immersive display.  
 575

## 576 5 Experimental Results

577  
 578 To thoroughly evaluate the impact of sensory conflict caused by remapping of spatial head-hand relations, we examined  
 579 the effects of remapping on different target objects (i.e., head-camera and hand-robot-arm), attributes (i.e., offset and  
 580 deflection), and intensity (i.e., large and small mapping parameters) on spatial perception and interaction behavior. We  
 581 also compared the effects of various remapping scenarios.  
 582

583 Since most data did not follow a normal distribution according to the Shapiro-Wilks test, medians were used to  
 584 represent the user data. Boxplots were used to visualize the data distribution of each metric, and tables ranked the  
 585 impact of each remapping situation. Among them, we employed SPSS's built-in post-Friedman pairwise comparison  
 586 method to assess significant differences between remapping targets, attributes, and intensity, based on Dunn's method  
 587 with Bonferroni correction [21]. This method in SPSS automatically adjusts p-values, keeping the significance level at  
 588 0.05. Moreover, we used Wilcoxon signed-rank tests to determine the significant differences between each remapping  
 589 situation and baseline (no offset and deflection).  
 590  
 591

### 592 5.1 Comparison of Different Remapping Targets

593  
 594 The remapping was applied to two target objects: the head and the hands. The impact of the remapping targets can  
 595 be revealed by comparing the different conditions set in this study. This section provides a statistical analysis of the  
 596 metrics: four perceptual bias rates (location, angle, depth, distance) from tasks 2 and 3; two trajectory deviations  
 597 (navigation, suturing) from tasks 1 and 4; six scores from the questions of NASA-TLX; and four completion time of  
 598 tasks. Additionally, significant differences between conditions were analyzed.  
 599  
 600  
 601  
 602

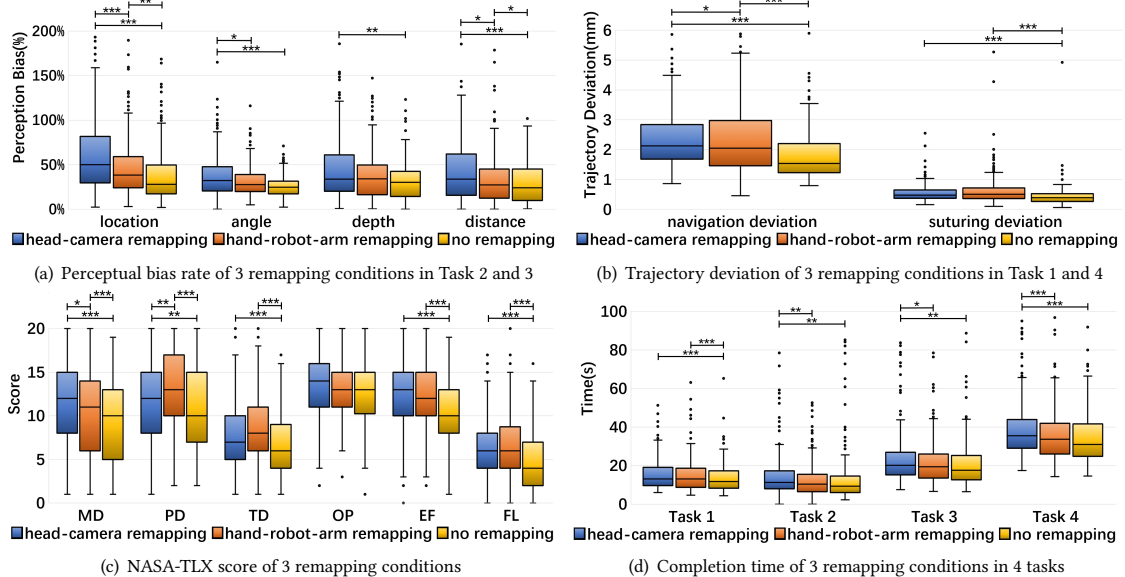


Fig. 5. Boxplots of 4 metric performances in three experimental conditions

The Friedman test results showed significant effects on: location bias rate ( $\chi^2(2) = 55.358, p < 0.001$ ), angle bias rate ( $\chi^2(2) = 16.358, p < 0.001$ ), depth bias rate ( $\chi^2(2) = 10.658, p = 0.005$ ), distance bias rate ( $\chi^2(2) = 24.758, p < 0.001$ ), navigation deviation in task 1 ( $\chi^2(2) = 96.533, p < 0.001$ ), and suturing deviation in task 4 ( $\chi^2(2) = 37.525, p < 0.001$ ). For NASA-TLX, significant differences were found in mental demand ( $\chi^2(2) = 64.266, p < 0.001$ ), physical demand ( $\chi^2(2) = 43.486, p < 0.001$ ), time demand ( $\chi^2(2) = 50.491, p < 0.001$ ), effort ( $\chi^2(2) = 57.922, p < 0.001$ ), frustration ( $\chi^2(2) = 65.870, p < 0.001$ ), and completion time in task 1 ( $\chi^2(2) = 30.608, p < 0.001$ ), task 2 ( $\chi^2(2) = 16.425, p < 0.001$ ), task 3 ( $\chi^2(2) = 12.175, p = 0.002$ ), and task 4 ( $\chi^2(2) = 25.908, p < 0.001$ ).

The boxplot (Figure 5) illustrates the data distribution and significant differences across conditions, with \* representing  $p < 0.05$ , \*\* representing  $p < 0.01$ , and \*\*\* representing  $p < 0.001$ .

Overall, compared to no remapping, different remapping targets had varying impacts on task performance. Head-camera remapping has the biggest perception bias rates, navigation deviation, mental load, and completion time. Hand-robot-arm remapping has the biggest suturing deviation and physical load.

## 5.2 Comparison of Different Remapping Attributes and Intensities

The remapping attributes are categorized into offset and deflection, while the intensities are divided into strong and weak. Thus, we further divided the two remapping conditions into the following groups: strong head-camera offset (SHCO), weak head-camera offset (WHCO), strong head-camera deflection (SHCD), weak head-camera deflection (WHCD), strong head-camera deflection (SHRO), weak head-camera deflection (WHRO), strong hand-robot-arm deflection (SHRD), weak hand-robot-arm deflection (WHRD), and no deflection (NOD).

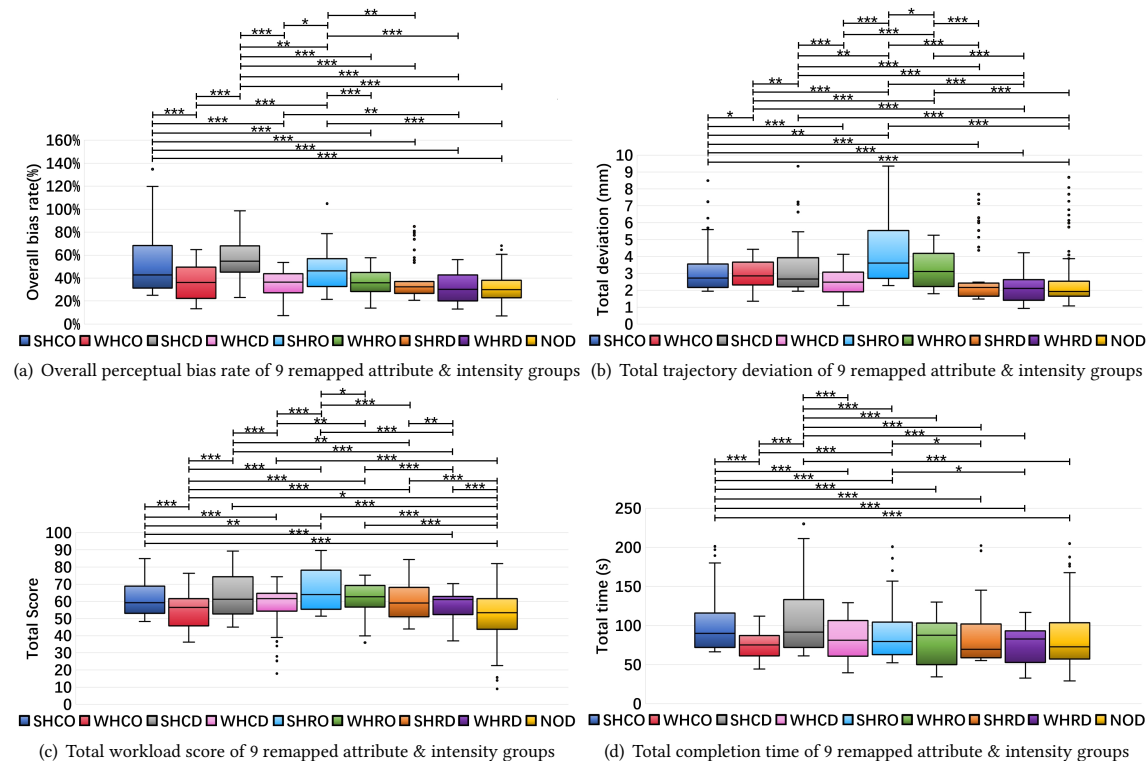


Fig. 6. Boxplots of 4 metric performances in 9 groups grouped by remapping attribute and intensity

(WHCD), strong hand-robot-arm offset (SHRO), weak hand-robot-arm offset (WHRO), strong hand-robot-arm deflection (SHRD), and weak hand-robot-arm deflection (WHRD). Together with no offset and deflection (NOD), a total of 9 groups are formed. Among them, strong and weak are determined by dividing the offset/deflection parameter range (5mm-15mm or 10°-30°) into two and checking whether the experimentally recorded parameter is in the smaller interval (5mm-10mm or 10°-20°) or the larger interval (10mm-15mm or 20°-30°).

Additionally, we averaged the 4 perceptual bias rates (location, angle, depth, and distance) to calculate the overall perceptual bias rate. We summed the navigation and suturing deviations to obtain the total trajectory deviation. The total workload score was calculated using the method outlined in the original paper of NASA-TLX [34], and the total completion time was derived by summing the time for 4 tasks.

Friedman test results indicated significant effects of conditions on the overall perceptual bias rate ( $\chi^2(8) = 245.324, p < 0.001$ ), total trajectory deviation ( $\chi^2(8) = 291.378, p < 0.001$ ), total workload score ( $\chi^2(8) = 374.886, p < 0.001$ ), and total completion time ( $\chi^2(8) = 196.604, p < 0.001$ ). The boxplot (Figure 6) illustrates the data distribution and significant differences across the different remapping attributes and intensities, where \* indicates  $p < 0.05$ , \*\* indicates  $p < 0.01$ , and \*\*\* indicates  $p < 0.001$ .

Overall, for the same remapping target and attribute, strong remapping performs worse than weak remapping. The head-camera deflection performs worse than its offset, while the hand-robot-arm offset performs worse than its deflection. Strong head-camera deflection results in the largest overall perceptual bias rate and total trajectory deviation, whereas strong hand-robot-arm offset leads to the highest total workload and completion time. No remapping and weak hand-robot-arm deflection tend to perform the best.

### 5.3 Comparison Between Different Remapping Situations and No Remapping Situation

This section evaluates the bias rate of location, angle, depth, and distance, total trajectory deviation, total completion time, and total workload. Only the four perception bias rates are not combined, as different remapping directions may

Table 3. Ranking of the impact level of 18 remapping situations compared to the no remapping situation

No.	Remapping situations	Location		Angle		Depth		Distance		Trajectory		Time		Workload	
		MD	Sig.	MD	Sig.	MD	Sig.	MD	Sig.	MD	Sig.	MD	Sig.	MD	Sig.
1	CDC/C	28.7%	**	12.3%	***	4.8%	*	14.8%	***	0.910	***	16.3	***	8.5	**
2	CDU/D	19.0%	*	13.5%	***	11.7%	**	6.1%	*	0.629	**	11.9	**	8.2	***
3	CDL/R	27.5%	*	13.1%	**	3.7%	**	7.9%	*	0.756	**	16.0	***	7.8	**
4	COF/B	21.3%	*	3.1%	/	3.7%	**	6.2%	*	0.891	**	12.8	*	4.8	***
5	ROU-D	25.3%	*	1.4%	/	1.2%	/	12.5%	*	2.287	**	13.5	*	17.0	***
6	COU/D	17.6%	*	4.2%	/	3.8%	*	10.5%	*	0.715	**	14.0	*	4.8	*
7	ROL-R	22.7%	*	2.2%	/	7.6%	/	16.4%	*	1.151	*	18.7	*	9.3	**
8	COL/R	14.9%	*	4.0%	/	-1.7%	/	3.9%	**	0.908	**	7.9	*	2.7	/
9	ROF-B	3.4%	/	3.9%	/	11.4%	**	2.3%	/	1.047	*	7.6	*	14.0	**
10	ROF/B	14.8%	/	3.5%	/	17%	**	7.5%	/	1.726	*	5.8	/	13.0	**
11	ROU/D	10.0%	/	-2.1%	/	3.8%	/	11.6%	*	1.382	*	11.0	*	8.5	**
12	ROL/R	16.6%	*	-2.2%	/	-3.8%	/	9.9%	/	0.987	*	7.6	/	7.8	**
13	RDL/R	6.8%	/	19%	*	4.9%	/	-6.2%	/	0.014	/	7.1	/	8.5	**
14	RDC/C	6.4%	/	4.3%	/	-4.1%	/	2.2%	/	0.135	/	-1.6	/	8.8	**
15	RDL-R	5.3%	/	3.5%	/	1.0%	/	-4.1%	/	0.393	/	4.7	/	6.7	*
16	RDC-C	5.0%	/	4.9%	/	-3.9%	/	-1.5%	/	0.313	/	-0.8	/	4.0	/
17	RDU/D	12.4%	/	1.4%	/	3.2%	/	-3.6%	/	-0.228	/	7.8	/	4.3	/
18	RDU-D	2.6%	/	-1.0%	/	2.2%	/	0.4%	/	-0.062	/	9.9	/	4.0	/

729 affect spatial perception in various directions. Using the Wilcoxon signed-rank test, we compared each remapping  
730 situation with the no-remapping situation. To better illustrate the various impacts of remapping situations, we ranked  
731 them by their impact size, as shown in Table 3. In the table, *MD* indicates the difference in medians between a remapping  
732 situation and the no-remapping situation for a specific metric, and *Sig.* indicates the significance of the difference (\*  
733 represents  $p < 0.05$ , \*\* represents  $p < 0.01$ , \*\*\* represents  $p < 0.001$ , green, blue and red backgrounds to highlight them  
734 respectively). The ranking strategy is based on the total number of \* across all metrics; if two conditions have the same  
735 number of \*, we further compare their *MD* values for each metric, with the situation having larger *MD* in more metrics  
736 ranked higher.  
737  
738

739 Overall, head-camera deflection has the greatest impact, especially when the camera deflects clockwise or counter-  
740 clockwise. Hand-robot-arm deflection has the smallest impact, particularly in situations where "one robot-arm deflects  
741 to clockwise, the other to counterclockwise," "two robot-arms deflect up/down," and "one robot-arm deflects to up, the  
742 other to down." Situations where the two robot arms offset in opposite directions typically ranked higher than situations  
743 with same-direction offset, while opposite-direction deflection situations generally ranked lower than same-direction  
744 deflection situations.  
745  
746

## 747 6 Discussion

748

749 The perceptual impact primarily stems from multisensory integration and conflicts, which can be effectively reflected  
750 in the spatial perception bias rates in Tasks 2 and 3. The behavioral effects are more complex, involving errors due  
751 to perceptual biases and physical factors such as increased physical exertion and limited joint flexibility caused by  
752 remapping. Therefore, this section first discusses the sensory conflicts and physical impacts caused by remapping  
753 separately. Then, we explore the broader value and implications of this study. Finally, we analyze the limitations of the  
754 paper and suggest directions for future work.  
755

756 Moreover, this study is exploratory and did not involve pre-formulated hypotheses before the experiment. Therefore,  
757 all discussions in this section provide exploratory insights.  
758  
759

### 760 6.1 Sensory Conflicts Impact from Remapping of Head-Hand Relations

761 6.1.1 *General impact and mechanism speculation.* As the study only involved robotic arm movements without whole-  
762 view movement, and no participants reported motion sickness during interviews, it can be inferred that the vestibular  
763 contribution was minimal. The primary sensory conflict caused by the remapping of head-hand relations is thus identified  
764 as a visual-proprioceptive conflict. Overall, remapping disrupts the natural alignment between human perception of the  
765 body and the environment. Compared to scenarios without remapping, we found that the visual-proprioceptive conflict  
766 caused by remapping reduced the accuracy of spatial perception and interaction behaviors, increased task completion  
767 time, and added cognitive load, significantly affecting participants' perception, cognition, and behavior. Moreover, we  
768 observed significant differences in the effects of remapping intensity. Smaller remapping parameters were easier to  
769 adapt to and had less impact on perception, cognition, and behavior, while larger remapping parameters disrupted  
770 multisensory integration more severely, increasing control difficulty and error.  
771  
772

773 Based on experimental results, observations, interviews, and sensory integration theory, we speculate that participants  
774 faced a perception-cognition-behavior mechanism under remapping. The mismatch between the visual representation  
775 of the head-hand relationship and proprioception led to confusion in sensory integration, making it difficult for users  
776 to accurately judge spatial positions, hand operations, or even movement directions. Remapping required users to  
777 adapt to the new head-hand relationship, with cognition having to process inconsistent sensory information. This  
778  
779  
780

781 adaptation process increased cognitive load, as the brain needed to resolve conflicting sensory inputs and coordinate  
782 them, leading to longer task completion times and requiring more attention to complete the same tasks. To cope with  
783 visual-proprioceptive conflict, users tended to adjust their behavior to correct the misalignment, leading to reduced  
784 precision and deviation in movement trajectories, and increased physical load, especially in fine surgical operations.  
785

786  
787 *6.1.2 Sensory Conflict Impact of Head-Camera Remapping.* We found that the sensory conflict had particularly strong  
788 effects when the remapping's target, attribute, and intensity were strong head-camera deflection. From observations  
789 and interviews, we discovered that camera deflection visually altered the movement direction of participants' physical  
790 hand motions. The direction sensed by the participant's proprioception did not align with the robotic arm's motion  
791 direction, which distinguished it from other remapping situations. For example, in the 'camera deflects to clockwise'  
792 situation, the participant's hand moved vertically upward, but the robotic arm moved toward the upper left in the view.  
793 Similarly, in the situations where of camera deflected to other direction, participants experienced distortion in the  
794 hand's movement in non-deflection axes. This change in the head-hand motion coordinate system caused strong spatial  
795 perception and motion control difficulties for the participants. Some users reported, "I kept trying to adapt and control  
796 the robotic arm to move in the direction I intended, which wasn't easy."  
797

798  
799 Moreover, we found that camera offset situations also affected spatial perception, though to a lesser extent than  
800 deflection situations. Among them, the 'camera is offset to forward/backward' situation had notable effects. This was  
801 primarily because when the camera offsets forward, the robotic arm appears closer to the camera, making the arm's size  
802 and movement seem larger in the view. Conversely, when the camera offsets backward, the robotic arm appears farther  
803 away, making its size and movement appear smaller in the view. This separation between the view and the hands  
804 affects the precision of integrating visual and proprioceptive signals, which in turn impacts the accuracy and difficulty  
805 of estimating spatial movements. Similarly, offset in other directions of the camera also affect hand-eye coordination  
806 precision. Additionally, this sensory conflict seems to influence certain cognitive aspects, such as body ownership.  
807 Some users reported, "I feel like I'm controlling my body from a third-person perspective, and at times, it feels like this  
808 robotic avatar isn't even me."  
809

810  
811  
812 *6.1.3 Sensory Conflict Impact of Hand-robot-arm Remapping.* In contrast to head-camera remapping, hand-robot-arm  
813 remapping did not affect the view or hand motion direction, resulting in less impact on spatial perception. According  
814 to Table 3, the offset of the robotic arm only influenced position-related metrics, while deflection of the robotic arm  
815 only affected angular perception, suggesting that remapping's effect may be more pronounced when the attribute of  
816 remapping (offset or deflection) aligns with the attribute of spatial perception (translation or rotation). Interestingly,  
817 we found that when the offset direction of the robotic arm aligned with the hand movement direction of the spatial  
818 perception tasks, the perception bias rate was significant. This finding reveals the directional influence of visual-  
819 proprioceptive conflict on perception bias.  
820

## 821 822 823 **6.2 Physical Impact from Remapping of Head-Hand Relations**

824  
825 We find that remapping introduced physical limitations, increasing physical load and further exacerbating interaction  
826 trajectory deviations. These limitations were mainly due to behavioral compensations, including eye movement  
827 compensation (for head-camera remapping) and hand movement compensation (for hand-robotic-arm remapping).  
828

829  
830 *6.2.1 Physical Impact of Head-Camera Remapping.* Specifically, camera offset and deflection shifted the operation area  
831 and robotic arm from the center of the view, requiring participants to slightly rotate their eyes to refocus on them for  
832



833 accurate interaction. For example, when the camera was offset or deflected upward, the operation area and robotic arms  
834 shifted downward in the view, requiring participants to look slightly downward to refocus. Interestingly, the workload  
835 caused by upward/downward camera offsets and deflects was greater than that caused by left/right offsets and deflects.  
836 We speculate that this is because horizontal eye movements are not obstructed by the eyelids, and people tend to make  
837 horizontal eye movements more frequently than vertical ones in daily life. As a result, the horizontal field of view is  
838 wider than the vertical one, making it easier to maintain stable focus after horizontal movements [43, 49].  
839  
840

841  
842 *6.2.2 Physical Impact of Hand-robot-arm Remapping.* We also found that hand-robot-arm remapping caused the highest  
843 physical workload, especially in cases where the robotic arm was offset. This is because the offset requires compensatory  
844 hand movements to maintain visually accurate interactions of robotic arms, and these compensations often result in  
845 greater hand/arm fatigue compared to when no compensations are needed. For example, in the case of downward  
846 offset, participants had to raise their hands higher to make the robotic arm return to the operational area, which often  
847 caused their arms to hover above the table, leading to the “gorilla arm” effect and thus increased fatigue [12]. In the  
848 case of upward offset, participants had to lower their hands for compensation, which sometimes caused their hands to  
849 be positioned lower than their elbows, further exacerbating fatigue. When the robotic arm was shifted forward, the  
850 hands had to move backward to maintain normal interaction, which could result in the hands hitting the VR headset,  
851 leading to more cautious control and increased physical load.  
852  
853

854 Moreover, situations where the two robotic arms were offset in opposite directions often resulted in a higher workload  
855 than when they were offset in the same direction. We speculate that this is because opposite-direction offsets place  
856 greater demands on hand coordination and trigger larger visual-proprioceptive conflicts. For instance, when the left  
857 robotic arm is offset left and the right robotic arm is offset right, participants’ compensatory movements could result in  
858 crossed hands (Figure 4(e)); whereas when the left robotic arm is offset right and the right robotic arm is offset left, the  
859 compensatory movements could result in a wider gap between the hands.  
860  
861

862 Interestingly, contrary to the results of offsets, same-direction deflections of the robotic arms generally had a  
863 significant impact on workload, while opposite-direction deflections did not. We speculate that this is due to the  
864 asymmetry in the flexibility of wrist rotation. For example, left-hand offsets to the right or deflects to counterclockwise  
865 are easier, while offsets to the left or deflects to clockwise are more difficult; similarly, right-hand offsets to the left  
866 or deflects to clockwise are easier, while offsets to the right or deflects to counterclockwise are more difficult. This  
867 asymmetry leads to one hand experiencing more difficulty in compensatory movements when both hands are deflected  
868 in the same direction, resulting in increased workload. In contrast, opposite-direction deflections offer two possibilities:  
869 either both hands experience difficult compensatory movements, or both hands find the compensations easy. These  
870 random possibilities may balance each other out, resulting in no significant impact on workload.  
871  
872

873 Additionally, we found that the two hand-robot-arm remapping situations involving upward/downward deflections  
874 had the smallest impact on workload across all scenarios. We speculate that this is because compensatory movements  
875 in upward or downward rotations are generally easier to perform.  
876  
877

### 878 **6.3 Research Value and Insights**

879  
880 The study of head-hand relation remapping in immersive telesurgery holds significant research value and offers insights  
881 in multiple areas, particularly in understanding multisensory integration mechanisms, improving surgical accuracy,  
882 optimizing operational experience, and designing new sensory intervention methods or teleoperation systems.  
883  
884

885 First, this paper is the first to identify the discrete remapping of spatial head-hand relations commonly found in  
886 immersive telesurgery systems. It systematically reveals the dual sensory conflict and physical impacts caused by  
887 remapping and proposes potential causes and mechanisms. This advances our understanding of how the perceptual  
888 system handles conflicting information, providing new perspectives for researching multisensory integration and  
889 perception-action compensation mechanisms.

891 Second, accuracy and safety are critical in immersive telesurgery systems. The remapping can affect the surgeon's  
892 spatial perception and operational precision with surgical tools and internal structures. The findings of this study,  
893 along with the ranking of the impacts of various remapping situations (Table 3), help identify remapping scenarios that  
894 surgeons should note or avoid to improve surgical precision and safety. For instance, if the camera needs to be deflected  
895 due to constraints within the patient's internal structures, the deflection angle should be minimized, or alternative  
896 remapping with lower impact, as indicated by the ranking, should be used to mitigate effects on perception, cognition,  
897 and behavior.

900 Third, by understanding the various influencing factors of remapping (e.g., target, attributes, intensity, situations) and  
901 their respective impact levels, designers of telesurgery systems can implement intervention measures to help surgeons  
902 maintain operational stability and accuracy under remappings. Intervention methods may include using visual and  
903 haptic augmentation techniques to guide correct perception and action, providing alerts when behavior deviations  
904 are detected or when remapping situations have a substantial impact, or designing motion compensation algorithms  
905 for robot arms to correct behavioral errors. Additionally, adaptive algorithms could be developed to reconstruct the  
906 hand-robot-arm relationship by automatically aligning the robot arms to the hands when feasible.

909 Fourth, immersive telesurgery systems are not only used in actual surgical procedures but are also widely applied  
910 in the training of surgeons. Studying the remapping impact on surgical operations can provide valuable insights  
911 for designing surgical training systems. By simulating different remapping situations, trainee surgeons can better  
912 adapt to teleoperation, improving their perceptual and operational accuracy when encountering remapping in real  
913 surgeries. Moreover, the findings can help in designing more effective training tasks. For example, designers could  
914 gradually increase the complexity of remapping during training to help surgeons adapt to sensory conflicts and varying  
915 operational environments. This will accelerate their learning process and enhance their performance in real surgeries.

918 Fifth, although the robot arms are consistent with the embodied actions of the human arms, the robot avatar may  
919 not foster a high level of body ownership. Studies have shown that stronger body ownership over the avatar enhances  
920 control over it [64]. Therefore, system designers could consider using AR technology to render the robot arms in  
921 the view as hand-holding surgical instruments. They might also consider leveraging the rubber hand illusion [17] by  
922 controlling one robot arm to stroke the other before the surgical interaction begins while one hand simultaneously  
923 strokes the other. This synchronous visual-tactile sensory stimulation could enhance body ownership.

925 Sixth, the results and findings regarding the remapping of head-hand relations are generalizable beyond the field  
926 of surgery. They can be extended to various application scenarios, such as teleoperating non-humanoid robots or  
927 controlling non-humanoid avatars in VR, where head-hand relations are also broken.

## 929 6.4 Limitations and Future Work

931 *6.4.1 Limitations.* Although this study systematically explores the remapping effects of spatial head-hand relations on  
932 perception, cognition, and behavior in the context of immersive telesurgery systems, there are still some limitations.

934 This research simulates the telesurgery system using a VR environment, rather than testing in a real surgical setting.  
935 While VR can effectively reproduce some features of immersive teleoperation, real surgeries may involve more complex

factors such as actual force feedback, tactile sensations, and the dynamic properties of surgical instruments, which are not fully reflected in this study.

Although the study designed 18 types of remapping situations, more complex and diverse remapping situations may occur in actual practice, such as the superposition of head-camera remapping and hand-robot-arm remapping.

This study primarily focuses on conflicts between visual and proprioceptive information, neglecting the influence of other sensory inputs such as tactile feedback. In real teleoperated surgeries, tactile feedback plays a critical role in operational precision and stability.

Although human sensory integration processes and mechanisms are generally similar, the use of non-surgeon participants might influence the results. For example, surgeons' experience, operational skills, and ability to adapt to sensory conflicts may affect their response to remapping.

**6.4.2 Future Work.** In the future, we plan to validate these findings in real telesurgery systems by collaborating with surgeons to assess the specific impacts of different remapping situations on spatial perception and operational behavior. This will provide more practical guidance for remapping.

We will also further investigate the integration and conflicts of multiple senses (such as vestibular and tactile senses) to reveal how to design sensory feedback more effectively under multisensory conditions, reducing conflicts caused by remapping and optimizing system design.

Additionally, we will explore how operators gradually adapt to sensory conflicts caused by remapping through training, designing effective training mechanisms to accelerate the adaptation process. Research will focus on how to use progressive remapping adjustments in virtual training environments to help operators more quickly adapt to complex operational scenarios in real surgeries.

Finally, we will also combine intelligent control algorithms with remapping research to develop adaptive telesurgery robotic systems. These systems would automatically adjust the head-hand relative relationship based on real-time data during the operation, alleviating sensory conflicts and reducing physical strain.

## 7 Conclusion

This study systematically examines the remapping effects of spatial head-hand relation in immersive telesurgery, revealing its significant impact on perception, cognition, and physical load. We found that head-camera remapping leads to the greatest spatial perception bias, particularly with strong deflection, while hand-robot-arm remapping results in increased physical limitations, especially with strong offset. These findings highlight the role of visual-proprioceptive conflicts and compensatory actions induced by remapping. Our research provides valuable insights for optimizing telesurgery systems, improving surgical training, and mitigating sensory conflicts to enhance surgical performance.

## References

- [1] Firas Abi-Farraj, Bernd Henze, Alexander Werner, Michael Panzirsch, Christian Ott, and Máximo A Roa. 2018. Humanoid teleoperation using task-relevant haptic feedback. In *2018 IEEE/RSJ International Conference on Intelligent Robots and Systems (IROS)*. IEEE, 5010–5017.
- [2] Parastoo Abtahi, Mar Gonzalez-Franco, Eyal Ofek, and Anthony Steed. 2019. I'm a giant: Walking in large virtual environments at high speed gains. In *Proceedings of the 2019 CHI Conference on Human Factors in Computing Systems*. 1–13.
- [3] Bart BGT Alberts, Luc PJ Selen, Giovanni Bertolini, Dominik Straumann, W Pieter Medendorp, and Alexander A Tarnutzer. 2016. Dissociating vestibular and somatosensory contributions to spatial orientation. *Journal of neurophysiology* 116, 1 (2016), 30–40.
- [4] Ruben Alonso, Alessandro Bonini, Diego Reforgiato Recupero, and Lucio Davide Spano. 2022. Exploiting virtual reality and the robot operating system to remote-control a humanoid robot. *Multimedia Tools and Applications* 81, 11 (2022), 15565–15592.
- [5] Mehran Anvari, Craig McKinley, and Harvey Stein. 2005. Establishment of the world's first telerobotic remote surgical service: for provision of advanced laparoscopic surgery in a rural community. *Annals of surgery* 241, 3 (2005), 460–464.

- 989 [6] Noorin Suhaila Asjad, Haley Adams, Richard Paris, and Bobby Bodenheimer. 2018. Perception of height in virtual reality: a study of climbing stairs. In *Proceedings of the 15th acm symposium on applied perception*. 1–8.
- 990 [7] Salah Bazzi and Dagmar Sternad. 2020. Human control of complex objects: towards more dexterous robots. *Advanced Robotics* 34, 17 (2020), 1137–1155.
- 992 [8] Norbert Bischof and Eckart Scheerer. 1970. Systems analysis of optic-vestibular interaction in the perception of verticality. *Psychologische Forschung* 34 (1970), 99–181.
- 993 [9] Johannes Bodner, Florian Augustin, Heinz Wykypiel, John Fish, Gilbert Muehlmann, Gerold Wetscher, and Thomas Schmid. 2005. The da Vinci robotic system for general surgical applications: a critical interim appraisal. *Swiss medical weekly* 135, 4546 (2005), 674–674.
- 994 [10] J Bodner, H Wykypiel, G Wetscher, and T Schmid. 2004. First experiences with the da Vinci™ operating robot in thoracic surgery. *European Journal of Cardio-thoracic surgery* 25, 5 (2004), 844–851.
- 995 [11] Luke Bölling, Niklas Stein, Frank Steinicke, and Markus Lappe. 2019. Shrinking circles: Adaptation to increased curvature gain in redirected walking. *IEEE transactions on visualization and computer graphics* 25, 5 (2019), 2032–2039.
- 996 [12] Sebastian Boring, Marko Jurmu, and Andreas Butz. 2009. Scroll, tilt or move it: using mobile phones to continuously control pointers on large public displays. In *Proceedings of the 21st Annual Conference of the Australian Computer-Human Interaction Special Interest Group: Design: Open 24/7*. 161–168.
- 1000 [13] Cynthia Breazeal and Brian Scassellati. 2002. Challenges in building robots that imitate people. (2002).
- 1001 [14] Lionel Bringoux, Vincent Nougier, Ludovic Marin, Pierre-Alain Barraud, and Christian Raphael. 2003. Contribution of somesthetic information to the perception of body orientation in the pitch dimension. *The Quarterly Journal of Experimental Psychology Section A* 56, 5 (2003), 909–923.
- 1002 [15] Kjell Brunnström, Elijs Dima, Tahir Qureshi, Mathias Johanson, Mattias Andersson, and Mårten Sjöström. 2020. Latency impact on quality of experience in a virtual reality simulator for remote control of machines. *Signal Processing: Image Communication* 89 (2020), 116005.
- 1003 [16] Chenyang Cai, Jian He, and Tianren Luo. 2023. Using Redirection to Create a Swimming Experience in VR for the Sitting Position. In *Companion Proceedings of the 28th International Conference on Intelligent User Interfaces*. 68–71.
- 1004 [17] Shivei Cheng, Yang Liu, Yuefan Gao, and Zhanxun Dong. 2024. “As if it were my own hand”: inducing the rubber hand illusion through virtual reality for motor imagery enhancement. *IEEE Transactions on Visualization and Computer Graphics* (2024).
- 1005 [18] Gilles Clement, Marie-Jose Fraysse, and Olivier Deguine. 2009. Mental representation of space in vestibular patients with otolithic or rotatory vertigo. *Neuroreport* 20, 5 (2009), 457–461.
- 1006 [19] Medcaroid Corporation. 2020. SYSTEM hinotori Robotic Assisted Surgery System PRODUCT Medcaroid. <https://www.medcaroid.com/en/product/hinotori/>. (2020).
- 1007 [20] M Diana and JJBJoS Marescaux. 2015. Robotic surgery. *Journal of British Surgery* 102, 2 (2015), e15–e28.
- 1008 [21] Olive Jean Dunn. 1964. Multiple comparisons using rank sums. *Technometrics* 6, 3 (1964), 241–252.
- 1009 [22] Natalia Dużmańska, Paweł Strojny, and Agnieszka Strojny. 2018. Can simulator sickness be avoided? A review on temporal aspects of simulator sickness. *Frontiers in psychology* 9 (2018), 2132.
- 1010 [23] Marc O Ernst and Martin S Banks. 2002. Humans integrate visual and haptic information in a statistically optimal fashion. *Nature* 415, 6870 (2002), 429–433.
- 1011 [24] Marc O Ernst and Heinrich H Bühlhoff. 2004. Merging the senses into a robust percept. *Trends in cognitive sciences* 8, 4 (2004), 162–169.
- 1012 [25] Syafizwan Faroque, Ben Horan, Husaini Adam, Mulyoto Pangestu, and Matthew Joordens. 2016. Haptic technology for micro-robotic cell injection training systems—A review. *Intelligent automation & soft computing* 22, 3 (2016), 509–523.
- 1013 [26] Elisa R Ferrè, Adrian JT Alsmith, Patrick Haggard, and Matthew R Longo. 2021. The vestibular system modulates the contributions of head and torso to egocentric spatial judgements. *Experimental Brain Research* 239, 7 (2021), 2295–2302.
- 1014 [27] Juan Manuel Florez, Jérôme Szewczyk, and Guillaume Morel. 2012. An impedance control strategy for a hand-held instrument to compensate for physiological motion. In *2012 IEEE International Conference on Robotics and Automation*. IEEE, 1952–1957.
- 1015 [28] Cinzia Freschi, Vincenzo Ferrari, Franca Melfi, Mauro Ferrari, Franco Mosca, and Alfred Cuschieri. 2013. Technical review of the da Vinci surgical telemanipulator. *The International Journal of Medical Robotics and Computer Assisted Surgery* 9, 4 (2013), 396–406.
- 1016 [29] Vicent Girbes-Juan, Vinicius Schettino, Yiannis Demiris, and Josep Tornero. 2020. Haptic and visual feedback assistance for dual-arm robot teleoperation in surface conditioning tasks. *IEEE Transactions on Haptics* 14, 1 (2020), 44–56.
- 1017 [30] Simone Grassini, Karin Laumann, Virginia de Martin Topranin, and Sebastian Thorp. 2021. Evaluating the effect of multi-sensory stimulations on simulator sickness and sense of presence during HMD-mediated VR experience. *Ergonomics* 64, 12 (2021), 1532–1542.
- 1018 [31] Tamás Haidegger, József Sándor, and Zoltán Benyó. 2011. Surgery in space: the future of robotic telesurgery. *Surgical endoscopy* 25 (2011), 681–690.
- 1019 [32] George B Hanna, Sami M Shimi, and Alfred Cuschieri. 1998. Randomised study of influence of two-dimensional versus three-dimensional imaging on performance of laparoscopic cholecystectomy. *The Lancet* 351, 9098 (1998), 248–251.
- 1020 [33] Nazim Haouchine, Jeremie Dequidt, Igor Peterlik, Erwan Kerrien, Marie-Odile Berger, and Stephane Cotin. 2014. Towards an accurate tracking of liver tumors for augmented reality in robotic assisted surgery. In *2014 IEEE International Conference on Robotics and Automation (ICRA)*. IEEE, 4121–4126.
- 1021 [34] SG Hart. 1988. Development of NASA-TLX (Task Load Index): Results of empirical and theoretical research. *Human mental workload/Elsevier* (1988).
- 1022 [35] Daigo Hayashi, Kazuyuki Fujita, Kazuki Takashima, Robert W Lindeman, and Yoshifumi Kitamura. 2019. Redirected jumping: Imperceptibly manipulating jump motions in virtual reality. In *2019 IEEE Conference on Virtual Reality and 3D User Interfaces (VR)*. IEEE, 386–394.

- [36] Nobuyuki Hinata, Raizo Yamaguchi, Yoshito Kusuhara, Hiroomi Kanayama, Yasuo Kohjimoto, Isao Hara, and Masato Fujisawa. 2022. Hinotori surgical robot system, a novel robot-assisted surgical platform: preclinical and clinical evaluation. *International Journal of Urology* 29, 10 (2022), 1213–1220.
- [37] Robert W Holloway and Sarfraz Ahmad. 2012. Robotic-assisted surgery in the management of endometrial cancer. *Journal of Obstetrics and Gynaecology Research* 38, 1 (2012), 1–8.
- [38] Wooju Jeong, Sung Yul Park, Enrique Ian S Lorenzo, Cheol Kyu Oh, Woong Kyu Han, and Koon Ho Rha. 2009. Laparoscopic partial nephrectomy versus robot-assisted laparoscopic partial nephrectomy. *Journal of endourology* 23, 9 (2009), 1457–1460.
- [39] Sungchul Jung, Christoph W Borst, Simon Hoermann, and Robert W Lindeman. 2019. Redirected jumping: Perceptual detection rates for curvature gains. In *Proceedings of the 32nd Annual ACM Symposium on User Interface Software and Technology*. 1085–1092.
- [40] Jihad H Kaouk, Ali Khalifeh, Shahab Hillyer, Georges-Pascal Haber, Robert J Stein, and Riccardo Autorino. 2012. Robot-assisted laparoscopic partial nephrectomy: step-by-step contemporary technique and surgical outcomes at a single high-volume institution. *European urology* 62, 3 (2012), 553–561.
- [41] Julian Keil, Dennis Edler, Denise O’Meara, Annika Korte, and Frank Dickmann. 2021. Effects of virtual reality locomotion techniques on distance estimations. *ISPRS International Journal of Geo-Information* 10, 3 (2021), 150.
- [42] Konstantina Kilteni, Jean-Marie Normand, Maria V Sanchez-Vives, and Mel Slater. 2012. Extending body space in immersive virtual reality: a very long arm illusion. *PLoS one* 7, 7 (2012), e40867.
- [43] Hiromi Kobayashi and Shiro Kohshima. 1997. Unique morphology of the human eye. *Nature* 387, 6635 (1997), 767–768.
- [44] Ryan B Kochanski, Joseph M Lombardi, Joseph L Laratta, Ronald A Lehman, and John E O’Toole. 2019. Image-guided navigation and robotics in spine surgery. *Neurosurgery* 84, 6 (2019), 1179–1189.
- [45] Ognjan I Kolev. 2019. Self-Motion Versus Environmental-Motion Perception Following Rotational Vestibular Stimulation and Factors Modifying Them. *Frontiers in Neurology* 10 (2019), 162.
- [46] Klas Kronander and Aude Billard. 2013. Learning compliant manipulation through kinesthetic and tactile human-robot interaction. *IEEE transactions on haptics* 7, 3 (2013), 367–380.
- [47] Eike Langbehn, Paul Lubos, Gerd Bruder, and Frank Steinicke. 2017. Bending the curve: Sensitivity to bending of curved paths and application in room-scale vr. *IEEE transactions on visualization and computer graphics* 23, 4 (2017), 1389–1398.
- [48] David Allen Larson. 2010. Artificial Intelligence: Robots, avatars, and the demise of the human mediator. *Ohio St. J. on Disp. Resol.* 25 (2010), 105.
- [49] Won June Lee, Ji Hong Kim, Yong Un Shin, Sunjin Hwang, and Han Woong Lim. 2019. Differences in eye movement range based on age and gaze direction. *Eye* 33, 7 (2019), 1145–1151.
- [50] Maëlis Lefebvre, João Bolina Rei, Elena Contreras, Raphaëlle N Roy, and Vsevolod Peysakhovich. 2022. Body tilt impacts operators’ perception of remote object’s orientation. In *International Astronautical Congress 2022*.
- [51] Ming Li and Russell H Taylor. 2004. Spatial motion constraints in medical robot using virtual fixtures generated by anatomy. In *IEEE International Conference on Robotics and Automation, 2004. Proceedings. ICRA’04. 2004*, Vol. 2. IEEE, 1270–1275.
- [52] Yi-Jun Li, Frank Steinicke, and Miao Wang. 2022. A comprehensive review of redirected walking techniques: Taxonomy, methods, and future directions. *Journal of Computer Science and Technology* 37, 3 (2022), 561–583.
- [53] Koeun Lim, Faisal Karmali, Keyvan Nicoucar, and Daniel M Merfeld. 2017. Perceptual precision of passive body tilt is consistent with statistically optimal cue integration. *Journal of neurophysiology* 117, 5 (2017), 2037–2052.
- [54] Wen P Liu, Sureerat Reaugamornrat, Anton Deguet, Jonathan M Sorger, Jeffrey H Siewerdsen, Jeremy Richmon, and Russell H Taylor. 2013. Toward intraoperative image-guided transoral robotic surgery. *Journal of robotic surgery* 7 (2013), 217–225.
- [55] Christophe Lopez, Christelle Bachofner, Manuel Mercier, and Olaf Blanke. 2009. Gravity and observer’s body orientation influence the visual perception of human body postures. *Journal of vision* 9, 5 (2009), 1–1.
- [56] Sudhir Srivastava Innovations Pvt. Ltd. 2023. SSI Mantra – SS Innovations International Inc. <https://ssinnovations.com/ssi-mantra/>. (2023).
- [57] Tianren Luo, Zhenxuan He, Chenyang Cai, Teng Han, Zhigeng Pan, and Feng Tian. 2022. Exploring Sensory Conflict Effect Due to Upright Redirection While Using VR in Reclining & Lying Positions. In *Proceedings of the 35th Annual ACM Symposium on User Interface Software and Technology*. 1–13.
- [58] Tianren Luo, Zehao Liu, Zhigeng Pan, and Mingmin Zhang. 2019. A virtual-real occlusion method based on gpu acceleration for mr. In *2019 IEEE Conference on Virtual Reality and 3D User Interfaces (VR)*. IEEE, 1068–1069.
- [59] Tianren Luo, Mingmin Zhang, Zhigeng Pan, Zheng Li, Ning Cai, Jinda Miao, Youbin Chen, and Mingxi Xu. 2020. Dream-experiment: a MR user interface with natural multi-channel interaction for virtual experiments. *IEEE Transactions on Visualization and Computer Graphics* 26, 12 (2020), 3524–3534.
- [60] Mark McGill, Aidan Kehoe, Euan Freeman, and Stephen Brewster. 2020. Expanding the bounds of seated virtual workspaces. *ACM Transactions on Computer-Human Interaction (TOCHI)* 27, 3 (2020), 1–40.
- [61] Medtronic. 2021. Products and system Medtronic (UK). <https://www.medtronic.com/covidien/en-gb/robotic-assisted-surgery/hugo-ras-system/products-and-system.html>. (2021).
- [62] Sarmad Mehrdad, Fei Liu, Minh Tu Pham, Arnaud Lelevé, and S Farokh Atashzar. 2020. Review of advanced medical telerobots. *Applied Sciences* 11, 1 (2020), 209.

- 1093 [63] K Moorthy, Y Munz, A Dosis, J Hernandez, S Martin, F Bello, T Rockall, and A Darzi. 2004. Dexterity enhancement with robotic surgery. *Surgical*  
1094 *Endoscopy and Other Interventional Techniques* 18 (2004), 790–795.
- 1095 [64] Ingrid A Odermatt, Karin A Buetler, Nicolas Wenk, Özhan Özen, Joaquin Penalver-Andres, Tobias Nef, Fred W Mast, and Laura Marchal-Crespo. 2021.  
1096 Congruency of information rather than body ownership enhances motor performance in highly embodied virtual reality. *Frontiers in neuroscience*  
1097 15 (2021), 678909.
- 1098 [65] Adrian Park, Gyusung Lee, F Jacob Seagull, Nora Meenaghan, and David Dexter. 2010. Patients benefit while surgeons suffer: an impending  
1099 epidemic. *Journal of the American College of Surgeons* 210, 3 (2010), 306–313.
- 1100 [66] Cristian Patras, Mantas Cibulskis, and Niels Christian Nilsson. 2022. Body warping versus change blindness remapping: A comparison of two  
1101 approaches to repurposing haptic proxies for virtual reality. In *2022 IEEE Conference on Virtual Reality and 3D User Interfaces (VR)*. IEEE, 205–212.
- 1102 [67] Anastasia Pavlidou, Elisa Raffaella Ferrè, and Christophe Lopez. 2018. Vestibular stimulation makes people more egocentric. *Cortex* 101 (2018),  
1103 302–305.
- 1104 [68] Valeria I Petkova, Malin Björnsdotter, Giovanni Gentile, Tomas Jonsson, Tie-Qiang Li, and H Henrik Ehrsson. 2011. From part-to whole-body  
1105 ownership in the multisensory brain. *Current Biology* 21, 13 (2011), 1118–1122.
- 1106 [69] Christian Pfeiffer, Christophe Lopez, Valentin Schmutz, Julio Angel Duenas, Roberto Martuzzi, and Olaf Blanke. 2013. Multisensory origin of the  
1107 subjective first-person perspective: visual, tactile, and vestibular mechanisms. *PloS one* 8, 4 (2013), e61751.
- 1108 [70] Pragathi Praveena, Daniel Rakita, Bilge Mutlu, and Michael Gleicher. 2020. Supporting perception of weight through motion-induced sensory  
1109 conflicts in robot teleoperation. In *Proceedings of the 2020 ACM/IEEE International Conference on Human-Robot Interaction*. 509–517.
- 1110 [71] Nora Preuss and H Henrik Ehrsson. 2019. Full-body ownership illusion elicited by visuo-vestibular integration. *Journal of Experimental Psychology:*  
1111 *Human Perception and Performance* 45, 2 (2019), 209.
- 1112 [72] Reuben Rideaux, Katherine R Storrs, Guido Maiello, and Andrew E Welchman. 2021. How multisensory neurons solve causal inference. *Proceedings*  
1113 *of the National Academy of Sciences* 118, 32 (2021), e2106235118.
- 1114 [73] Michael Rietzler, Florian Geiselhart, Jan Gugenheimer, and Enrico Rukzio. 2018. Breaking the tracking: Enabling weight perception using perceivable  
1115 tracking offsets. In *Proceedings of the 2018 CHI Conference on Human Factors in Computing Systems*. 1–12.
- 1116 [74] Michael Rietzler, Florian Geiselhart, and Enrico Rukzio. 2017. The matrix has you: realizing slow motion in full-body virtual reality. In *Proceedings*  
1117 *of the 23rd ACM Symposium on Virtual Reality Software and Technology*. 1–10.
- 1118 [75] Michael Rietzler, Jan Gugenheimer, Teresa Hirzle, Martin Deubzer, Eike Langbehn, and Enrico Rukzio. 2018. Rethinking redirected walking: On the  
1119 use of curvature gains beyond perceptual limitations and revisiting bending gains. In *2018 IEEE international symposium on mixed and augmented*  
1120 *reality (ISMAR)*. IEEE, 115–122.
- 1121 [76] Hiroaki Sakoe and Seibi Chiba. 1978. Dynamic programming algorithm optimization for spoken word recognition. *IEEE transactions on acoustics,*  
1122 *speech, and signal processing* 26, 1 (1978), 43–49.
- 1123 [77] Hiroaki Sakono, Keigo Matsumoto, Takuji Narumi, and Hideaki Kuzuoka. 2021. Redirected walking using continuous curvature manipulation. *IEEE*  
1124 *Transactions on Visualization and Computer Graphics* 27, 11 (2021), 4278–4288.
- 1125 [78] Alexander Seitel, Markus Engel, Christof M Sommer, Boris A Radeleff, Caroline Essert-Villard, Claire Baegert, Markus Fangerau, Klaus H Fritzsche,  
1126 Kwong Yung, Hans-Peter Meinzer, et al. 2011. Computer-assisted trajectory planning for percutaneous needle insertions. *Medical physics* 38, 6Part1  
1127 (2011), 3246–3259.
- 1128 [79] Charles S Sherrington. 1907. On the proprioceptive system, especially in its reflex aspect. *Brain* 29, 4 (1907), 467–482.
- 1129 [80] Stine Maya Dreier Sørensen, Mona Meral Savran, Lars Konge, and Flemming Bjerrum. 2016. Three-dimensional versus two-dimensional vision in  
1130 laparoscopy: a systematic review. *Surgical endoscopy* 30 (2016), 11–23.
- 1131 [81] Yunpeng Su, Xiaoqi Chen, Tony Zhou, Christopher Pretty, and Geoffrey Chase. 2022. Mixed reality-integrated 3D/2D vision mapping for intuitive  
1132 teleoperation of mobile manipulator. *Robotics and Computer-Integrated Manufacturing* 77 (2022), 102332.
- 1133 [82] Yun-Peng Su, Xiao-Qi Chen, Cong Zhou, Lui Holder Pearson, Christopher G Pretty, and J Geoffrey Chase. 2023. Integrating virtual, mixed, and  
1134 augmented reality into remote robotic applications: A brief review of extended reality-enhanced Robotic systems for Intuitive Telemanipulation and  
1135 Telemanufacturing tasks in Hazardous conditions. *Applied Sciences* 13, 22 (2023), 12129.
- 1136 [83] Intuitive Surgical. 2024. Da Vinci Robotic Surgical Systems Intuitive. <https://www.intuitive.com/en-us/products-and-services/da-vinci>. (2024).
- 1137 [84] Rob Surgical. 2023. Bitrack System - Rob Surgical. <https://www.robsurgical.com/bitrack-system/>. (2023).
- 1138 [85] Ryo Takata, Mitsugu Kanehira, Yoichiro Kato, Tomohiko Matsuura, Renpei Kato, Shigekatsu Maekawa, and Wataru Obara. 2021. Improvement of  
1139 three-dimensional motion sickness using a virtual reality simulator for robot-assisted surgery in undergraduate medical students: A prospective  
1140 observational study. *BMC Medical Education* 21 (2021), 1–7.
- 1141 [86] Russell Taylor, Pat Jensen, Louis Whitcomb, Aaron Barnes, Rajesh Kumar, Dan Stoianovici, Puneet Gupta, ZhengXian Wang, Eugene Dejuan, and  
1142 Louis Kavoussi. 1999. A steady-hand robotic system for microsurgical augmentation. *The International Journal of Robotics Research* 18, 12 (1999),  
1143 1201–1210.
- 1144 [87] Meta Technologies. 2022. Oculus Quest 2. <https://www.oculus.com/quest-2/>. (2022).
- 1145 [88] M Trope, Reuben R Shamir, Leo Joskowicz, Z Medress, G Rosenthal, Arnaldo Mayer, N Levin, A Bick, and Yigal Shoshan. 2015. The role of automatic  
1146 computer-aided surgical trajectory planning in improving the expected safety of stereotactic neurosurgery. *International journal of computer assisted*  
1147 *radiology and surgery* 10 (2015), 1127–1140.

- 1145 [89] P Van Bergen, W Kunert, and GF Buess. 1999. Three-dimensional (3-D) video systems: bi-channel or single-channel optics? *Endoscopy* 31, 09 (1999),  
1146 732–737.
- 1147 [90] David B Van de Merwe, Leendert Van Maanen, Frank B Ter Haar, Roelof JE Van Dijk, Nirul Hoeba, and Nanda Van der Stap. 2019. Human-robot  
1148 interaction during virtual reality mediated teleoperation: How environment information affects spatial task performance and operator situation  
1149 awareness. In *Virtual, Augmented and Mixed Reality. Applications and Case Studies: 11th International Conference, VAMR 2019, Held as Part of the 21st  
1150 HCI International Conference, HCII 2019, Orlando, FL, USA, July 26–31, 2019, Proceedings, Part II 21*. Springer, 163–177.
- 1151 [91] Thomas Van Gemert, Kasper Hornbæk, Jarrod Knibbe, and Joanna Bergström. 2023. Towards a bedder future: A study of using virtual reality while  
1152 lying down. In *Proceedings of the 2023 CHI Conference on Human Factors in Computing Systems*. 1–18.
- 1153 [92] Francesco Volonté, François Pugin, Pascal Bucher, Maki Sugimoto, Osman Ratib, and Philippe Morel. 2011. Augmented reality and image overlay  
1154 navigation with OsiriX in laparoscopic and robotic surgery: not only a matter of fashion. *Journal of Hepato-biliary-pancreatic Sciences* 18, 4 (2011),  
1155 506–509.
- 1156 [93] Breedveld Wentink. 2001. Eye-hand coordination in laparoscopy-an overview of experiments and supporting aids. *Minimally Invasive Therapy &  
1157 Allied Technologies* 10, 3 (2001), 155–162.
- 1158 [94] Bob G Witmer and Wallace J Sadowski Jr. 1998. Nonvisually guided locomotion to a previously viewed target in real and virtual environments.  
1159 *Human factors* 40, 3 (1998), 478–488.
- 1160 [95] Murphy Wonsick and Taskin Padir. 2020. A systematic review of virtual reality interfaces for controlling and interacting with robots. *Applied  
1161 Sciences* 10, 24 (2020), 9051.
- 1162 [96] Murphy Wonsick and Taşkın Padir. 2021. Human-humanoid robot interaction through virtual reality interfaces. In *2021 IEEE Aerospace Conference  
1163 (50100)*. IEEE, 1–7.
- 1164 [97] Tianyu Zhou, Qi Zhu, and Jing Du. 2020. Intuitive robot teleoperation for civil engineering operations with virtual reality and deep learning scene  
1165 reconstruction. *Advanced Engineering Informatics* 46 (2020), 101170.

1166  
1167  
1168  
1169  
1170  
1171  
1172  
1173  
1174  
1175  
1176  
1177  
1178  
1179  
1180  
1181  
1182  
1183  
1184  
1185  
1186  
1187  
1188  
1189  
1190  
1191  
1192  
1193  
1194  
1195  
1196